

Enhancing the conductivity of molecular electronic devices

Thijs Stuyver, Stijn Fias, Frank De Proft, Paul Geerlings, Yuta Tsuji, and Roald Hoffmann

Citation: *J. Chem. Phys.* **146**, 092310 (2017); doi: 10.1063/1.4972992

View online: <http://dx.doi.org/10.1063/1.4972992>

View Table of Contents: <http://aip.scitation.org/toc/jcp/146/9>

Published by the [American Institute of Physics](#)

Articles you may be interested in

[Destructive quantum interference in electron transport: A reconciliation of the molecular orbital and the atomic orbital perspective](#)

J. Chem. Phys. **146**, 092308092308 (2016); 10.1063/1.4972572

[Temperature dependent tunneling conductance of single molecule junctions](#)

J. Chem. Phys. **146**, 092311092311 (2017); 10.1063/1.4973318

[Structure dependent spin selectivity in electron transport through oligopeptides](#)

J. Chem. Phys. **146**, 092302092302 (2016); 10.1063/1.4966237

[Nonequilibrium diagrammatic technique for Hubbard Green functions](#)

J. Chem. Phys. **146**, 092301092301 (2016); 10.1063/1.4965825



**COMPLETELY
REDESIGNED!**

**PHYSICS
TODAY**

Physics Today Buyer's Guide
Search with a purpose.

Enhancing the conductivity of molecular electronic devices

Thijs Stuyver,^{1,2,a)} Stijn Fias,¹ Frank De Proft,¹ Paul Geerlings,¹ Yuta Tsuji,³ and Roald Hoffmann⁴

¹*QCMM Ghent–Brussels Alliance Group and Algemene Chemie, Vrije Universiteit Brussel, Pleinlaan 2, 1050 Brussels, Belgium*

²*Research Foundation-Flanders (FWO-Vlaanderen), Egmontstraat 5, 1000 Brussels, Belgium*

³*Education Center for Global Leaders in Molecular Systems for Devices, Kyushu University, Nishi-ku, Fukuoka 819-0395, Japan*

⁴*Department of Chemistry and Chemical Biology, Baker Laboratory, Cornell University, Ithaca, New York 14853, USA*

(Received 28 October 2016; accepted 12 December 2016; published online 28 December 2016)

We show in this work that conjugated π -electron molecular chains can, in quite specific and understood circumstances, become more conductive the longer they get, in contradiction to what would be expected intuitively. The analysis, done in the framework of the source and sink potential method, and supported by detailed transmission calculations, begins by defining “relative transmission,” an inherent measure of molecular conduction. This, in turn, for conjugated hydrocarbons, is related to a simple molecular orbital expression—the ratio of secular determinants of a molecule and one where the electrode contacts are deleted—and a valence bond idea, since these secular determinants can alternatively be expressed in terms of Kekulé structures. A plausible argument is given for relating the relative transmission to the weight of the diradical resonance structures in the resonance hybrid for a molecule. Chemical intuition can then be used to tune the conductivity of molecules by “pushing” them towards more or less diradical character. The relationship between relative transmission (which can rise indefinitely) and molecular transmission is carefully analyzed—there is a sweet spot here for engineering molecular devices. These new insights enable the rationalization of a wide variety of experimental and theoretical results for π -conjugated alternant hydrocarbons, especially the striking difference between extended oligophenylenes and related quinoid chains. In this context, oligo-*p*-phenylene macrocycles emerge as a potential molecular switch. *Published by AIP Publishing.* [<http://dx.doi.org/10.1063/1.4972992>]

I. INTRODUCTION

Much effort in the field of theoretical molecular electronics has been directed towards gaining insight into the remarkable phenomenon of quantum interference (QI).^{1–4} General strategies to increase the conductivity of molecules through structural modification have attracted less attention.^{5–8} In this work, we will explore just such strategies for a class of conjugated π -electron systems, even alternant hydrocarbons.

An alternant hydrocarbon is a planar π -electron system in which all the carbon atoms that take part in the conjugated system can be divided into two classes (e.g., labeled by zeros and stars, as shown in Fig. 1 for benzene) so that members of the two classes alternate and atoms of the same class are never next to one another.⁹ The alternant classification is one of the oldest in the theory of conjugated hydrocarbons; its consequences are mathematically and physically strong and, as we will show, retain their vitality in our time.

II. THEORY

We start from the Source and Sink Potential (SSP) method to obtain an expression for the transmission probability in a molecular electronic device (MED).^{10–12} The transmission probability through a molecule can be defined as the probability for an electron, which has entered the system, to travel through the molecule without being scattered. It can be related to the conductance with the help of the Landauer formula,¹³

$$G(E) = \frac{2e^2}{h} T(E), \quad (1)$$

where $G(E)$ and $T(E)$ are, respectively, the conductance of the molecule and the transmission probability of an electron traveling through the molecule at the energy level of E .

Although many researchers have been using the Non-Equilibrium Green's Function (NEGF) methodology¹³ to calculate transmission probabilities, in our theoretical development here we adopt the alternative Source and Sink Potential (SSP) method. The equivalency of the two methodologies has been explicitly demonstrated by Fowler *et al.*¹⁴ The expression for the transmission probability through a π -electron system connected to contacts at atoms r and s can be written as follows:^{11,12}

^{a)} Author to whom correspondence should be addressed. Electronic mail: Thijs.Stuyver@vub.ac.be

$$T_{r,s}(E) = \frac{4\tilde{\beta}^2 \sin^2 q(\Delta_{r,r}(E)\Delta_{s,s}(E) - \Delta(E)\Delta_{rs,rs}(E))}{\left|e^{-2iq}\Delta(E) - e^{-iq}\tilde{\beta}\Delta_{s,s}(E) - e^{-iq}\tilde{\beta}\Delta_{r,r}(E) + \tilde{\beta}^2\Delta_{rs,rs}(E)\right|^2}. \quad (2)$$

In this expression, Δ stands for the characteristic polynomial of the Hückel/tight-binding Hamiltonian matrix of the original molecule incorporated into the molecular electronic device (\mathbf{H}) in units of β (resonance integral between adjacent carbon atoms) with α (the on-site Coulomb integral) set to zero. The letters before and after the comma in the subscripts denote, respectively, the rows and columns omitted from the secular determinant that gives rise to this polynomial, so that

$$\Delta(E) = \det(\mathbf{E}\mathbf{1} - \mathbf{H}), \quad (3)$$

$$\Delta_{s,s}(E) = \det(\mathbf{E}\mathbf{1} - \mathbf{H})^{s,s}, \quad (4)$$

$$\Delta_{r,r}(E) = \det(\mathbf{E}\mathbf{1} - \mathbf{H})^{r,r}, \quad (5)$$

$$\Delta_{rs,rs}(E) = \det(\mathbf{E}\mathbf{1} - \mathbf{H})^{rs,rs}, \quad (6)$$

where $\mathbf{1}$ is the unit matrix. Furthermore, q denotes the wave vector of the Bloch wave passing through the system, and $\tilde{\beta}$ is defined as follows:

$$\tilde{\beta} = \frac{\beta_{MC}^2}{\beta_C}, \quad (7)$$

with β_{MC} being the resonance integral between the atom in the molecule at the point of attachment to the contact and the first atom of the contact, and β_C being the resonance integral between atoms in the molecule. A recapitulation of the derivation of this expression (Eq. (2)) can be found in the [supplementary material](#).

Around the Fermi level ($E = 0$), Eq. (2) can be simplified to^{11,12}

$$T_{r,s}(0) = \lim_{E \rightarrow 0} \frac{4\tilde{\beta}^2 (\Delta_{r,r}(E)\Delta_{s,s}(E) - \Delta(E)\Delta_{rs,rs}(E))}{\left|-\Delta(E) - i\tilde{\beta}\Delta_{s,s}(E) - i\tilde{\beta}\Delta_{r,r}(E) + \tilde{\beta}^2\Delta_{rs,rs}(E)\right|^2}. \quad (8)$$

As already mentioned above, we will focus in this work on even alternant hydrocarbons, where the number of starred and unstarred atoms is even. Coulson and Longuet-Higgins demonstrated that for this class of hydrocarbons, $\Delta_{r,r}$ and $\Delta_{s,s}$

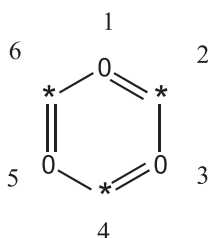


FIG. 1. The carbon atoms of benzene divided in two classes (0 and *).

are odd functions of the energy.¹⁵ Odd functions are by definition equal to zero at the origin, so $\Delta_{r,r}(0) = 0$ and $\Delta_{s,s}(0) = 0$, thus

$$T_{r,s}(0) = \lim_{E \rightarrow 0} \frac{-4\tilde{\beta}^2\Delta(E)\Delta_{rs,rs}(E)}{\left|-\Delta(E) + \tilde{\beta}^2\Delta_{rs,rs}(E)\right|^2}. \quad (9)$$

Since the denominator is now completely real, the absolute value signs can be taken care of simply as follows:

$$T_{r,s}(0) = \lim_{E \rightarrow 0} \frac{-4\tilde{\beta}^2\Delta(E)\Delta_{rs,rs}(E)}{\Delta^2(E) - 2\tilde{\beta}^2\Delta(E)\Delta_{rs,rs}(E) + \tilde{\beta}^4\Delta_{rs,rs}^2(E)}. \quad (10)$$

In the weak interaction limit ($\tilde{\beta} \rightarrow 0$), this expression can be further simplified to¹⁶

$$T_{r,s}(0) = \lim_{E \rightarrow 0} -4\tilde{\beta}^2 \left(\frac{\Delta_{rs,rs}(E)}{\Delta(E)} \right). \quad (11)$$

III. RELATIVE TRANSMISSION

We now introduce a quantity, which we call “relative transmission,” which is defined as follows:

$$T_{r,s}^{rel}(0) = \lim_{E \rightarrow 0} -\frac{\Delta_{rs,rs}(E)}{\Delta(E)}. \quad (12)$$

Note that $T_{r,s}^{rel}(0)$ is positive because $\Delta_{rs,rs}(0)$ and $\Delta(0)$ have the opposite sign (or are equal to zero).¹⁷ The first reason for introducing this definition is convenience, as will become clear below. The second reason for doing this is that this quantity is the closest one can get to an inherent measure of the molecular conductance, independent of the type and strength of the connection to the contacts. The characteristic polynomials depend only on the electronic structure of the isolated molecule, and in turn on its topology and connectivity. This enables us to make a comparison between the relative transmissions of different types of molecules.

In Secs. IV–X we will continue to work with this relative transmission instead of the complete expression for the transmission probability.

IV. KEKULÉ STRUCTURES AND RELATIVE TRANSMISSION

What we say in this section is familiar to the graph-theoretical community. Who, we hope, will forgive us for the pedagogical exposition to introduce this subject. In the early days of MO theory, it was important to establish a connection between valence bond (VB) structures and MO energies. Though much of the impetus has faded, the relationship remains important. For even alternant hydrocarbons that do not contain $4n$ -membered rings, it is possible to relate $\Delta(0)$ to the number of Kekulé structures, K , of the original molecule ($\Delta(0) = (-1)^{N/2} K^2$) and $\Delta_{rs,rs}(0)$ to the number of Kekulé

The computation of such a determinant of an $n \times n$ matrix involves a similar procedure of matrix element selection as the one used in the analysis above in exploring the relation between the Hamiltonian matrix and the Kekulé (or diradical) structures. In the Leibniz formula (Eq. (16)),²² a determinant can be equated to a sum of terms, each of these being a combination of matrix elements so that every row and column is selected only once in that term,

$$\det(A) = \sum_{\sigma \in S_n} \text{sgn}(\sigma) \prod_{i=1}^n a_{i,\sigma_i}. \quad (16)$$

Here the sum is computed over all permutations σ of the set $\{1, 2, \dots, n\}$. The set of all such permutations is denoted by S_n . For each permutation σ , $\text{sgn}(\sigma)$ denotes the signature of σ (+1 or -1), and a_{i,σ_i} denotes the matrix element in the i th row and σ_i th column.

When the determinant in Eq. (15) is calculated in this way for $E = 0$, the only terms differing from zero in Eq. (16) will be the ones where only matrix elements with value 1 have been selected. For both the upper right and lower left block of the determinant in Eq. (15), the number of non-zero terms that can be obtained this way is equal to K , as we demonstrated in the analysis above. For all even alternant hydrocarbons except $4n$ -membered rings (or hydrocarbons containing $4n$ -membered rings), these terms can simply be added according to Eq. (16) since $\text{sgn}(\sigma)$ will be the same for every term.^{23–25} So, the determinant of each of both these blocks will be proportional to K . Since the determinant of a block matrix can be expressed as the product of the determinants of its blocks, this means that $\det(\mathbf{H})$, or $\Delta(0)$, will be proportional to K^2 .

Let us think about a situation where it is impossible to draw any full Kekulé structures for an even alternant hydrocarbon. Such a situation occurs when the molecule is diradical, tetraradical, hexaradical, and so on. In this case, the characteristic polynomial will contain at least two explicit E factors. As such, the resulting characteristic polynomial will be equal to zero when $E \rightarrow 0$, and this zero root will have a multiplicity of at least two. The exact multiplicity depends on the number of radical centers in the structure.

In short, the connection established above demonstrates that there is a one-to-one relationship between the number of Kekulé structures of a molecule and the corresponding characteristic polynomial evaluated at the origin. As a result, when it is impossible to draw a Kekulé resonance structure for an even alternant hydrocarbon ($K = 0$), the characteristic polynomial evaluated at the origin will evidently be zero

($\Delta(0) = 0$). The same is true of course for the “deleted molecule” ($K_{-rs} = 0 \rightarrow \Delta_{rs,rs}(0) = 0$). When it is impossible to draw a Kekulé structure, the number of radical centers in the radical structure corresponds to the multiplicity of the zero root in the characteristic polynomial.

V. FOUR LIMITING SITUATIONS

Returning to the expression for the relative transmission in terms of characteristic polynomials, $T_{r,s}^{rel}(0) = -\Delta_{rs,rs}(0)/\Delta(0)$, four distinct situations can now be distinguished:

1. If $\Delta(0) \neq 0$ and $\Delta_{rs,rs}(0) = 0$, then the relative transmission will go to zero.
2. If $\Delta(0) \neq 0$ and $\Delta_{rs,rs}(0) \neq 0$, then the relative transmission will be a real, non-zero number differing from zero.
3. If $\Delta(0) = 0$ and $\Delta_{rs,rs}(0) \neq 0$, then the relative transmission will go to infinity.
4. If $\Delta(0) = 0$ and $\Delta_{rs,rs}(0) = 0$, then the relative transmission can either be zero, be a real, non-zero number, or go to infinity.

Of these four situations, the first and second have been explored in detail before.^{1,2,4,6,7,26} The starting point for both is an even alternant hydrocarbon (which do not contain $4n$ -membered rings) for which a Kekulé resonance structure can be drawn (e.g., benzene; $K \neq 0 \rightarrow \Delta(0) \neq 0$). The first situation corresponds to configurations of contacts that demonstrate destructive quantum interference (e.g., contacts connected *meta* on benzene). If the starting molecule considered is an alternant hydrocarbon, it is impossible to draw a Kekulé structure for the r and s deleted system in this situation ($K_{-rs} = 0$). As a result, unpaired electrons are present in this “deleted” molecule (making it a diradical or two separate monoradicals), leading to energy levels at the Fermi level ($E = 0$), namely, non-bonding molecular orbitals (NBMOs), and a characteristic polynomial ($\Delta_{rs,rs}$) that is zero at this E -value. As a result, the relative transmission will be zero at the Fermi level, leading to quantum interference (see Fig. 4(a)).

The second situation corresponds to configurations of contacts that do not lead to quantum interference (e.g., *para* on benzene, see Fig. 4(b)). For these systems, we can construct Kekulé structures for both the original and the “deleted” molecular graphs ($K \neq 0$; $K_{-rs} \neq 0$), so both characteristic polynomials differ from zero at the Fermi energy ($E = 0$), leading to a defined (and non-zero) relative transmission.

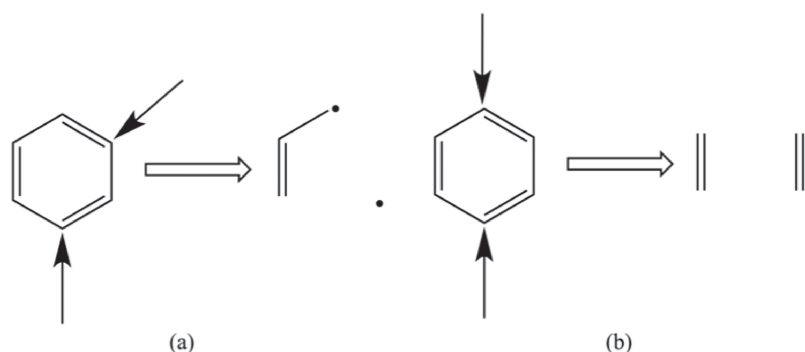


FIG. 4. (a) Deletion of carbon atoms in the 2nd and 4th positions for benzene leads to only radical structures and no Kekulé structures, so connection of contacts on these positions leads to quantum interference close to the Fermi level. (b) Deletion of carbon atoms in the 1st and 4th positions for benzene leads to one Kekulé structure, so connection of contacts on these positions gives rise to a defined relative transmission differing from zero.

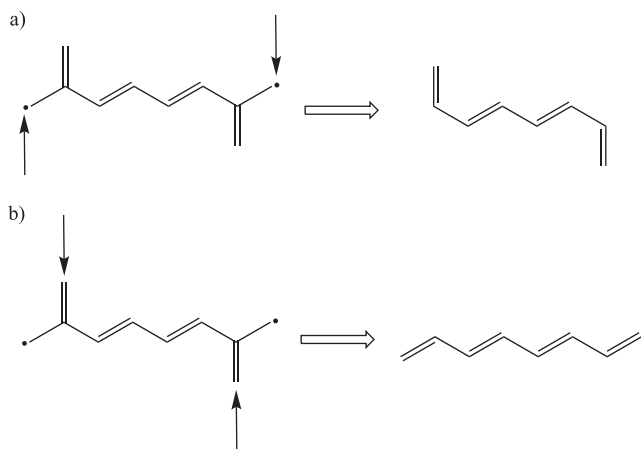


FIG. 5. Deletion of the radical centers in a diradical molecule leads to a Kekulé structure, so connection of contacts on these positions leads to an infinitely big relative transmission. (a) The contacts are attached to the radical sites, while in (b) the contacts are attached to the non-radical sites where the radicals can delocalize.

The starting point for the third and fourth situations is a (poly)radical so that $\Delta(0) = 0$ (e.g., trimethylenemethane). In the third situation, the original molecule has to be a diradical ($K = 0 \rightarrow \Delta(0) = 0$) and the “deleted molecule” has to have at least one Kekulé resonance structure ($K_{-rs} \neq 0$) so that $\Delta_{rs,rs} \neq 0$, leading to an infinitely big relative transmission. In order to go from a diradical to a molecule, for which one can draw a Kekulé structure, the radical centers have to disappear. A radical center can be made to disappear by deleting one of the carbon atoms to which that radical can delocalize. Two examples are shown in Fig. 5.

We are well aware of the difficulty of this situation ever being realized. Diradicals rarely have much kinetic persistence, even if they are detected. Attaching contacts to the radical sites, in order to study conductivity experimentally, will be very difficult. The situation is to be viewed as a limit, describing an approach to a diradical. In the second part of the paper, we will describe realistic, relatively stable molecules that do just this.

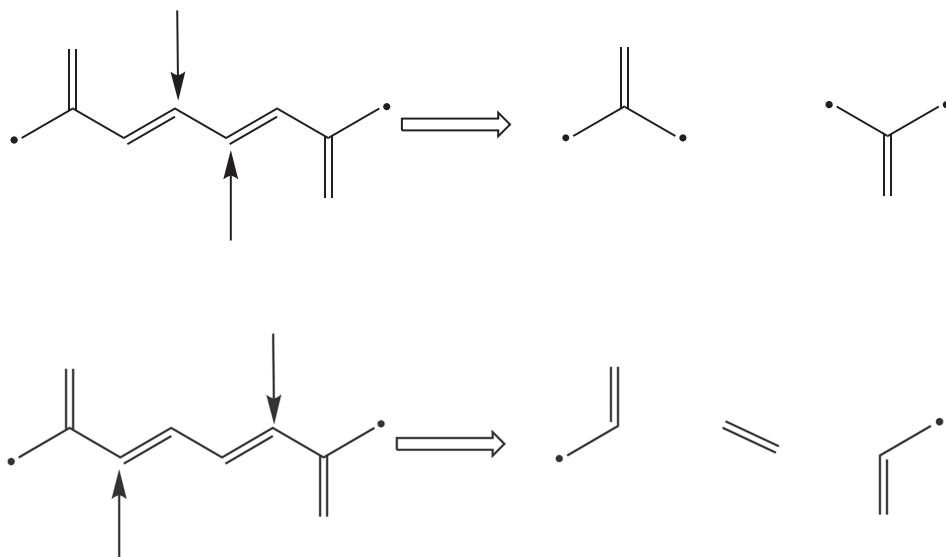


FIG. 6. If the number of radical centers increases after deletion, then connection of contacts on these positions gives rise to a quantum interference close to the Fermi level.

FIG. 7. If the number of radical centers stays the same after deletion, then connection of contacts on these positions gives rise to a defined (non-zero) transmission probability.

The fourth situation is the most exotic of all. In order for the relative transmission to go to zero in this situation, the original radical centers cannot disappear after deletion, and additional radical centers have to be formed. An example is given in Fig. 6.

Because of the earlier mentioned proportionality of the number of radical centers and the multiplicity of the zero root in the characteristic polynomial, if the number of radical centers in the deleted molecule is larger than the number of radical centers in the original molecule, the multiplicity of the zero roots in the numerator of Eq. (12) ($\Delta_{rs,rs}$) is higher than the multiplicity in the denominator (Δ).¹² The zero roots are associated with factors of E , not $E - x$, in the characteristic polynomials. Application of L'Hôpital's rule a sufficient number of times²⁷ gives rise to only zero roots in the numerator and a denominator differing from zero at the origin, thus devolving back into situation 1 (QI).

In order for the relative transmission to be a real, non-zero number, the original radical centers cannot disappear after deletion, but neither should new centers be formed. Fig. 7 shows an example.

This can be easily understood as follows. Because the number of radical centers remains the same, the multiplicity of the zero root in numerator and denominator of the expression for the relative transmission is equal,¹² and application of the L'Hôpital's rule leads to a defined fraction in the expression of the relative transmission. Thus this case devolves into situation 2.

The relative transmission in the fourth situation can only go to infinity if the starting molecule has more than 2 radical centers, where the “deleted molecule” has 2 radical centers less than the original one. Through the same reasoning as before, application of L'Hôpital's rule a sufficient number of times, this fourth case devolves into situation 3. Fig. 8 shows two examples.

The analyses of situations 3 and 4 lead to the conclusion that diradicals (and polyradicals) can have infinitely big relative transmission around the Fermi level if and only if the positions of the contacts are chosen on carbon atoms to

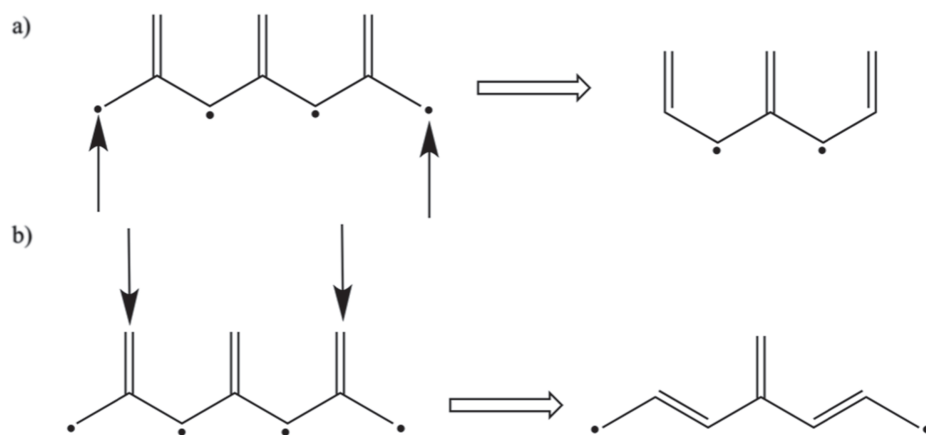


FIG. 8. If the number of radical centers drops after deletion, then connection of contacts on these positions gives rise to an infinitely big relative transmission.

which the radical centers can delocalize. If other positions are taken, the relative transmission either becomes a real, non-zero number or zero.

Before we go on, it is important to make three points. First we have glibly said “diradical.” We are fully aware of the complexity and richness of what might be called “the diradical situation.” Six microstates arise from the placing of two electrons into two degenerate or nearly degenerate orbitals—three singlets and a triplet.^{28,29} Depending on the symmetry, the singlets may or may not be subject to a first- or second-order Jahn-Teller distortion.³⁰ We will return to a detailed consideration of the behavior of the various diradical states elsewhere.

Second, the relationship between the characteristic polynomial and the number of Kekulé structures laid out above does not hold for $4n$ -membered rings (and hydrocarbons that contain such a ring), because the terms corresponding to the different Kekulé structures will cancel each other out in Eq. (16) in general.^{23–25} The simplest example of this class of molecules is cyclobutadiene (CBD). In the simple Hückel model, all resonance integrals are taken equal, corresponding to a perfect square geometry (D_{4h}) for CBD. Although it is possible to draw two completely equivalent Kekulé resonance structures for this molecule ($K = 2$), the molecule will be a diradical in this approximation, having two degenerate NBMOs at $E = 0$. A detailed analysis of the interesting transmission

possibilities offered up by substituted CBDs, some of which can be stabilized, is given in the [supplementary material](#).

Finally, the terminology of “infinite relative transmission” is guaranteed to make believers in the first law of thermodynamics blanch. We therefore turn to a detailed discussion of what this phrase implies.

VI. RELATIVE TRANSMISSION VS. TRANSMISSION PROBABILITY

How is the relative transmission of a molecule related to the actual transmission probability of the resulting molecular electronic device? Let us rewrite Eq. (10) by dividing both numerator and denominator by $\Delta^2(0)$

$$T_{r,s}(0) = \lim_{E \rightarrow 0} \frac{-4\tilde{\beta}^2 \frac{\Delta_{rs,rs}(E)}{\Delta(E)}}{1 - 2\tilde{\beta}^2 \frac{\Delta_{rs,rs}(E)}{\Delta(E)} + \tilde{\beta}^4 \frac{\Delta_{rs,rs}^2(E)}{\Delta^2(E)}}, \quad (17)$$

which is equivalent to

$$T_{r,s}(0) = \frac{4\tilde{\beta}^2 T_{r,s}^{rel}(0)}{1 + 2\tilde{\beta}^2 T_{r,s}^{rel}(0) + \tilde{\beta}^4 T_{r,s}^{rel^2}(0)}. \quad (18)$$

It is clear from Eq. (18) that the approximation leading to Eq. (11) is only valid when $\tilde{\beta}^2 T_{r,s}^{rel}(0)$ is sufficiently small so that the second and third terms in the denominator can be neglected. Only in this case the transmission probability is directly proportional to the relative transmission.

In the literature, β_{MC} values of 0.2 are commonly used for realistic junctions.^{1,2} Setting β_C to 1 then leads to a value for $\tilde{\beta}$ of 0.04 (see Eq. (7)). For such a value of $\tilde{\beta}$, Eq. (11) is a very good approximation up to relative transmission values of approximately 50. In Fig. 10, the change of the transmission probability with the value of the relative transmission is calculated according to Eq. (18), and plotted by a bold line. If the approximations hold, the slope should be $4\tilde{\beta}^2$. When $\tilde{\beta} = 0.04$, $4\tilde{\beta}^2 = 0.0064$, which is close to the numerically approximated value of 0.0055 (Fig. 9).

Even for much higher values than 50, the relative transmission remains a good indicator for the transmission probability. Even though the direct proportionality between the two quantities is now no longer valid, a higher relative transmission

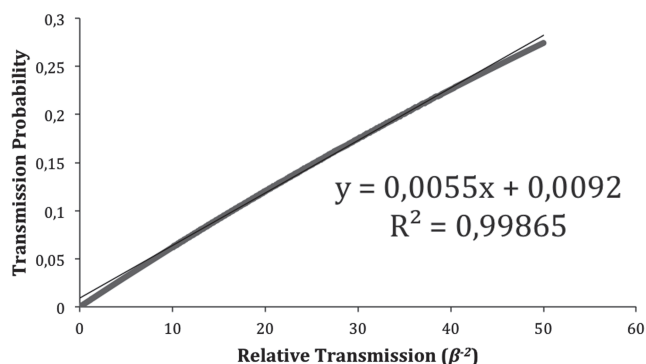


FIG. 9. Transmission probability as a function of the relative transmission (indicated by the bold line). $\tilde{\beta}$ was set at 0.04 (weak interaction), and the relative transmission was varied from 1 to 50.

will still result in a higher transmission probability, up to the point where a maximum ($T_{r,s}(0) = 1$) is achieved. This maximum value can be determined by setting the derivative of the transmission probability to the relative transmission to zero. The following analytical expression for the derivative can be obtained:

$$\frac{\partial T_{r,s}(0)}{\partial T_{r,s}^{rel}(0)} = \frac{4\tilde{\beta}^2 (1 + 2\tilde{\beta}^2 T_{r,s}^{rel}(0) + T_{r,s}^{rel^2}(0)) - 4\tilde{\beta}^2 T_{r,s}^{rel}(0) (2\tilde{\beta}^2 + 2\tilde{\beta}^4 T_{r,s}^{rel}(0))}{(1 + 2\tilde{\beta}^2 T_{r,s}^{rel}(0) + \tilde{\beta}^4 T_{r,s}^{rel^2}(0))^2} = \frac{4\tilde{\beta}^2 (1 - \tilde{\beta}^4 T_{r,s}^{rel^2}(0))}{(1 + 2\tilde{\beta}^2 T_{r,s}^{rel}(0) + \tilde{\beta}^4 T_{r,s}^{rel^2}(0))^2}. \quad (19)$$

Equating this expression to zero leads to a root at $T_{r,s}^{rel}(0) = 1/\tilde{\beta}^2$. Filling in the chosen value of $\tilde{\beta}$ means that a maximal transmission probability is obtained at a relative transmission of 625 ($1/0.04^2$). Beyond this maximum, the transmission probability will start decreasing with increasing relative transmission. This decrease however is very slow, leading to transmission probabilities still quite close to unity at relative transmission values well beyond 1000. This is illustrated graphically in Fig. 10.

The relative transmission as an indicator for the transmission probability only starts failing at the most extreme values for the relative transmission. When $\tilde{\beta}^2 T_{r,s}^{rel}(0)$ becomes sufficiently large, the third term in the denominator of Eq. (10) will predominate so that the first and second terms can be neglected, leading to

$$T_{r,s}(0) = \frac{4}{\tilde{\beta}^2 T_{r,s}^{rel}(0)}. \quad (20)$$

This demonstrates that in extreme cases where the relative transmission approaches infinity, the actual transmission probability becomes inversely proportional to the relative transmission even for the case of the weak interaction between the molecule and the contacts. For the construction of a realistic molecular device, the aim would then be to approach $T_{r,s}^{rel}(0) = 1/\tilde{\beta}^2$. This is the sweet spot.

As mentioned in Sec. V, the only type of molecules that can have a relative transmission approaching infinity is a perfect diradical or polyradical (corresponding to $\Delta = 0$). As we said, it is not easy to attach contacts to a diradical—most lack kinetic persistence. Also realistic analysis would need

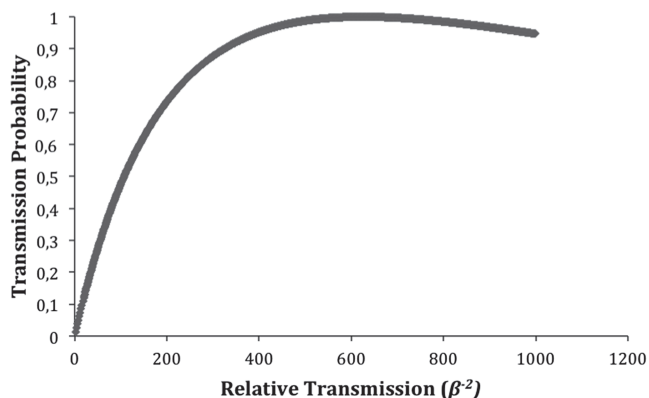


FIG. 10. Transmission probability as a function of the relative transmission. $\tilde{\beta}$ was set at 0.04 (relatively weak interaction), and the relative transmission was varied from 1 to 1000.

to consider the different available states (triplet, closed, and open-shell singlets) of a target diradical. In the remainder of our argument below, we will generally not consider such molecules. Instead, we will focus on closed-shell molecules for which diradical resonance structures have some weight, perhaps a substantial one, in the resonance hybrid.³¹ As long as we stay far enough away from a real diradical (and thus also from a potentially infinitely big relative transmission), the relative transmission remains a good indicator for the transmission probability.

Now that the relationship between relative transmission and transmission probability has been clarified, we will shift our focus to the main idea we want to explore in this paper, which that *chemical intuition can be used to tune the conductivity of molecules under a small bias by “pushing” a molecule towards more or less “diradical character.”* The four situations distinguished in Sec. V will be used as a starting point and we will mainly focus on the relative transmission. We will not explicitly make the link with the transmission probability at every single instance due to the direct proportionality we illustrated above.

A side note to be made is that whenever the diradical character of a molecule will be discussed throughout this text, we refer to the relative importance of the diradical resonance structures in the total resonance hybrid. For a detailed description of diradical(oid)s, we refer to some excellent work in the literature.^{28,29,32}

In a first stage, we focus on the simplest class of alternant hydrocarbons, linear polyenes.

VII. LINEAR POLYENES

Bond alternation explains the exponential drop-off in the relative transmission with increasing length for even linear polyenes.³³ Since an even carbon atom polyene has a single basic Kekulé structure ($K = 0$), we are in situation 1 or 2 of Section V; depending on the placement of the contacts, one has either QI or a definite transmission. If the electrodes are placed at the termini of the chain, and if there is no bond length alternation, the relative transmission will be unity, independently of the length of the wire.

This is in clear contradiction with experimental results, which all indicate an exponential drop-off of the conductance with the length.^{34,35} This expected behavior can, however, be retrieved computationally by taking into account the obvious, which is that the equal-length structure is not an energy minimum, but distorts exactly in the direction indicated by a Kekulé structure (Fig. 11 left, drawn for 8 carbons).³³

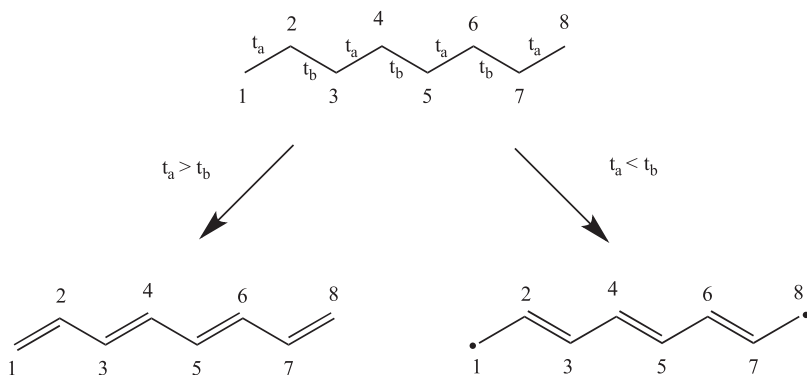


FIG. 11. Polyene skeleton with the resonance integrals (top). The dominant resonance structure with $t_a > t_b$ (lower left). An important (dominant) resonance structure with $t_a < t_b$ (lower right).

Defining t_a as the resonance integral between C_{2n-1} and C_{2n} and t_b as the resonance integral between C_{2n} and C_{2n+1} (Fig. 11 top) implies that $t_a > t_b$. Exponential decrease of the conductance with the length of the polyene is then obtained indeed.³³

What would happen if we could somehow invert this situation and take $t_a < t_b$? In that case, calculations indicate that an exponential *increase* in the relative transmission can be expected.³³

If we wish to describe this situation ($t_a < t_b$) by a resonance structure, we are drawn to one in which the double bonds come between the pairs of carbon atoms that are associated with the larger resonance integral, t_b . When we do this, an unpaired electron remains on each side of the chain (Fig. 11 right). This corresponds to a diradical resonance structure!

Working with our intuition (the full valence bond (VB) calculations will in time be done), the longer the polyene becomes for the $t_a < t_b$ case, the more weight will this diradical resonance structure get, because all those more favorable double bonds between atoms with a higher resonance integral would have to be broken in order to get rid of the two radical centers at the ends of molecule. As a result, connection of contacts at these chain end positions thus becomes increasingly reminiscent of situation 3 (the relative transmission increases).

For the other case, the normal one, $t_a > t_b$, the reverse happens—the longer the chain becomes, the smaller the weight of the extremely separated diradical resonance structure. This is what emerges from detailed calculations of Gu, Wu, and Shaik,^{36–38} sketched in the [supplementary material](#). Connection of the contacts at the chain end positions in this case resembles more and more situation 2, and, as mentioned, the relative transmission decreases (exponentially) with chain length.

This analysis for linear polyenes clearly illustrates that adjustments of the resonance integrals/bond distances provide an option to tune the diradical character and thus improve the transport properties of a molecule. Recent work by Proppe and Herrmann on the influence of bond stretching on the transmission probability points in the same direction.⁸ However, we have to face up to reality—it is very hard to control or influence in a chemical way the bond lengths in a polyene in the way we want, so that $t_a < t_b$. A better strategy to improve the conductance of a molecule might be to find a structural element that has the same effect as bond alternation on the weight of

diradical resonance structure in the resonance hybrid. Aromatic rings turn out to be good candidates for this.

VIII. MOLECULAR WIRES THAT DIFFER MARKEDLY

Consider the following two wires, oligo(*p*-phenyl) and oligo(pheno)-*p*-quinodimethane, and focus on the MED in which these molecules are connected to the contacts through the ends of the wires (Fig. 12).

Although these structures are exactly equivalent except for two terminal methylene groups, their chemical properties could not differ more. Recent calculations demonstrated completely opposite trends in the evolution of the transport properties with the length of the chains for these molecules.^{5,6} Our new insights into the relation between diradical character and relative transmission enable us to shed some new light on these results.

We start by considering the “monomers” of both wires first, benzene and *para*-quinodimethane (PQDM). For benzene, the formation of a *para*-diradical resonance structure (a single Dewar structure) effectively breaks the aromaticity of the system. The weight of that Dewar structure is actually substantial (10.2%; we thank Danovich and Shaik for a computation here).³⁹ As phenyl rings are added—for instance, in moving to biphenyl, terphenyl etc.—more and more aromatic benzene ring Kekulé structures would have to be broken to create an α - ω diradical (the radical sites at the ends of the chain). The weights of such diradical resonance structures should fall rapidly with chain length.

The situation is very different for the quinoid chain. First consider the “monomer,” *para*-quinodimethane, Fig. 13. In addition to the normal valence structure, the quinoid one at

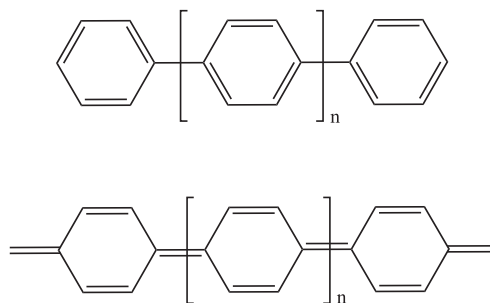


FIG. 12. oligo(*p*-phenyl) and oligo(pheno)-*p*-quinodimethane.

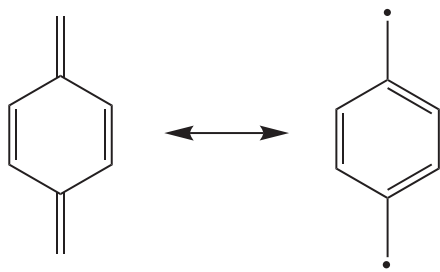


FIG. 13. The Kekulé structure and (stabilized) diradical resonance structure of *p*-quinodimethane.

the left-hand side of this figure, a diradical resonance structure can be drawn. The number of double bonds decreases here compared to the Kekulé structure, but aromaticity is gained. As such, we can expect an increase in the weight of this aromatically stabilized diradical resonance structure compared to the equivalent polyene. According to the VB calculations by Shaik and Danovich, the weight of these stabilized diradical resonance structures amount to 4.2% for the optimized geometry. That is not large—there are in fact two factors working in opposite directions to produce this weight. The number of electron shifts necessary to produce the diradical structure reduces its weight, while the aromaticity gained in the diradical increases it.

One can tune the contribution of this structure by equalizing the bond lengths in the central ring, thus increasing the aromaticity of the central hexagon. The weight increases to 17% when this is done (for details, see the [supplementary material](#)).³⁹

Other measures point towards a significant diradical character for PQDM. Based on the occupation of the lowest formally unoccupied natural orbital, Nakano and co-workers, for example, obtained a value for the diradical character of 15%.⁴⁰

We have probed the effect of the aromatic ring on the transmission probability by excising a hexatriene from the quinoid

structure of Fig. 13 (i.e., deleting one of the central ring double bonds), and calculating the transmission 1,4 vs 1,6 in that triene. It falls off with the number of intervening double bonds, as expected for a bond-alternated oligoene. We compared this with a similar transmission when the benzene ring is completed (i.e., the PQDM in Fig. 13). Then the corresponding transmission order is reversed—the longer path actually gives a bigger transmission probability. And the effect is augmented when benzene bond lengths are equalized. Details are given in the [supplementary material](#).

On extending the structures linearly, the trend is reinforced. In order to obtain a diradical resonance structure in biphenyl, two aromatic rings have to be broken. On the other hand, pheno-*p*-quinodimethane (also known as Chichibabin's hydrocarbon) gains two aromatic rings, making this resonance structure even more important in the resonance hybrid for this molecule than it was for the monomer (see Fig. 14). Steric effects between the phenyl rings (see discussion in [supplementary material](#)) enhance the differential behavior.

This trend persists as we move on to longer and longer wires. While the importance of the diradical resonance structures decreases with the length of the wire for oligo(*p*-phenylene), their importance increases for oligo(pheno)-*p*-quinodimethane. Calculation of the relative transmission around the Fermi level (see Fig. 15) in the simple Hückel model (all resonance integrals are set to be equal) leads to the conclusion that for oligo(*p*-phenylene) the relative transmission (and thus the conductance) drops exponentially with the length of the chain, whereas for oligo(pheno)-*p*-quinodimethane the relative transmission increases exponentially.^{5,6} Just as before, the importance of the diradical resonance structures in the resonance hybrid determines the conductivity of these molecules.

There is something very interesting about the large relative transmission calculated (greater than 1000 for $n = 5$). Recall here our discussion of the relation between transition

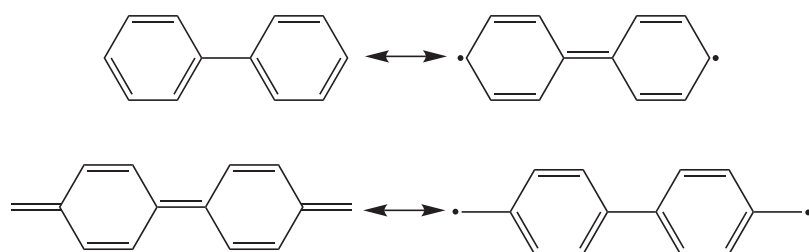


FIG. 14. The diradical resonance structures of biphenyl (top) and pheno-*p*-quinodimethane, or Chichibabin's hydrocarbon (bottom).

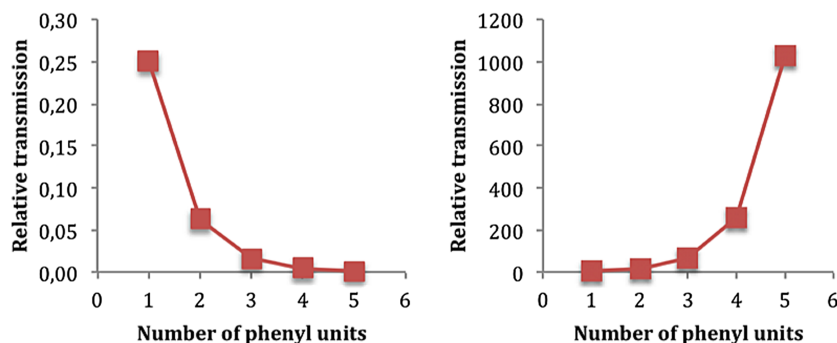


FIG. 15. The exponential decay of the relative transmission for oligo(*p*-phenylene) (left) and the exponential growth of the relative transmission for oligo(pheno)-*p*-quinodimethane (right) with an increasing number of phenyl units.⁶

probability and relative transmission, and its dependence on the amount of coupling between the molecule and the contacts. Given our assumptions, the maximum of the transmission probability should be located somewhere between the relative transmission values of tri- ($n = 4$) and tetra(pheno)-*p*-quinodimethane ($n = 5$).

Detailed DFT calculations (computational details in [supplementary material](#)) were performed to verify these predictions. The transmission spectra of both oligo(*p*-phenylene) and oligo(pheno)-*p*-quinodimethane are presented in the [supplementary material](#); a plot of the transmission probability at the Fermi level as a function of the length of the wires can be found in Fig. 16.

From this figure it can be clearly seen that as the chain becomes longer for oligo(*p*-phenylene), the transmission probability at the Fermi level decreases exponentially in accordance with our predictions. If we use a geometry in which all the benzene rings are forced to be in the same plane (denoted by PP'(n)), the decrease in transmission is less pronounced, but still exponential.

For oligo(pheno)-*p*-quinodimethane, the transmission probability across the molecule increases with the length of the chain up to tri(pheno)-*p*-quinodimethane ($n = 4$), after which it decreases. This also corresponds qualitatively to our predictions. The maximum in the transmission probability curve is already reached somewhat before $n = 4$ (see Fig. 16), because the coupling between the molecule and the contacts is set slightly stronger in these DFT calculations than the general estimate we have introduced at the Hückel level in Section VI ($\tilde{\beta} = 0.04$).

Our analysis leads to the conclusion that for oligo(pheno)-*p*-quinodimethane, the conductivity increases with the length of the molecule up to at least tri(pheno)-*p*-quinodimethane ($n = 4$). This startling result might come across as counterintuitive and unphysical. But, as we will detail later on, although these specific molecules have not yet been studied experimentally, experimental data for related classes of molecules^{41–43} appear to confirm our general assertion of the proportionality between the weight of diradical resonance structures in the resonance hybrid—and the role played by aromatic rings in driving this weight up (or down)—and the conductance of a molecule.

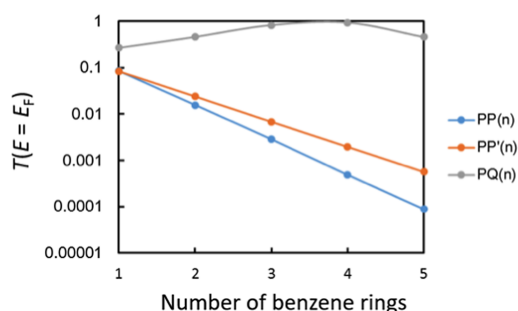


FIG. 16. Transmission probability at the Fermi level as a function of the number of benzene rings calculated for oligo(*p*-phenylene) (PP(n)) and oligo(pheno)-*p*-quinodimethane (PQ(n)). PP'(n) indicates oligo(*p*-phenylene) molecules optimized under the restriction that all the benzene rings are in the same plane.

IX. POLYCYCLIC AROMATICS—NANOGRAPHENES

The ideas introduced here relating the contribution of diradical resonance structures in the resonance hybrid to enhanced transmission can also be expanded to a related group of molecules, the polycyclic benzene-ring extensions of anthracene and phenanthrene, or “nanographenes.” In the electronic structures of these, as we examine possible diradical structures, any loss of aromaticity will come with an energetic penalty, diminishing the contribution of the diradical resonance structures to the resonance hybrid, compared to non-aromatic (bond-equalized) conjugated systems in which double bonds can be broken without a loss or gain of aromaticity. We need a measure of this penalty, and in the absence of complete VB calculations for the higher hydrocarbons, we choose to look at the experimental/theoretical value of the resonance or delocalization energy involved.^{44,45} For benzene this is 36 kcal/mol.

For anthracene, not all diradical structures are subject to the same energetic penalty anymore. Consider, for example, a positioning of the radical centers on opposite sides of the central ring (at carbons 9 and 10 in the conventional numbering scheme, Fig. 17). The energetic penalty in this case is strongly reduced because the loss of the aromaticity of the anthracene ring is almost completely compensated by a gain in aromaticity of two benzene rings (the resonance energy of anthracene is determined at 80 kcal/mol,⁴⁵ so the penalty is estimated to drop to approximately 8 kcal/mol).

All other diradical resonance structures for anthracene are associated with a far higher energetic penalty, since they lead either only to the gain of one naphthalene (resonance energy estimated to be 60 kcal/mol)⁴⁵ or a single benzene (see [supplementary material](#) for discussion). As a result, the 9,10-diradical resonance structure should be the main diradical contributor to the resonance hybrid and its relative weight likely will be higher than for the benzene resonance structure in which the radical centers are placed in *para*-position. As such, we can expect that, when contacts are placed at these positions, the relative transmission will be bigger than for *para*-connected benzene. These predictions have been confirmed both theoretically and experimentally.^{41–43}

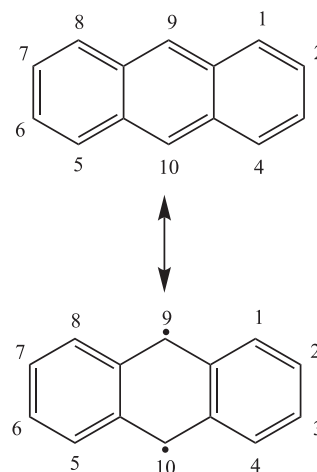


FIG. 17. The likely main diradical resonance structure of anthracene.

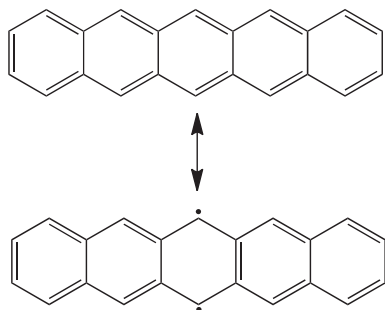


FIG. 18. The main diradical resonance structure expected for pentacene.

For pentacene (Fig. 18), a similarly stabilized diradical resonance structure can be drawn, this time with the formation of two naphthalene rings. For this resonance structure, the modification in the aromaticity pattern no longer leads to an energetic penalty in our line of reasoning, but to a stabilization. The loss of aromaticity of the pentacene ring (resonance energy estimated at 117 kcal/mol)⁴⁵ is more than compensated by the gain in aromaticity of the two naphthalene rings formed. Resonance structures with diradicals elsewhere on the zigzag edges will have larger penalties, lower weights.

As more benzene rings are attached, we can expect this trend to continue. The contribution of diradical resonance structures with radical centers on the zigzag edges to the resonance hybrid should increase, and as such the relative transmission increases when contacts are connected to those edges. The main driving force for this effect is the gradual decrease in the additional resonance energy when more benzene rings are added—in the table by Wiberg,⁴⁵ the additional resonance energy per benzene unit added decreases from 24 kcal/mol, on going from benzene to naphthalene, up to 18 kcal/mol on going from naphthalene to pentacene.

In the limit of an infinitely long polyacene, the diradical resonance structures should predominate,^{46–48} which leads to the conclusion that the HOMO-LUMO gap for such a molecule should be 0, corresponding to an infinitely big relative transmission. This is indeed what is observed for zigzag nanographene.^{49,50}

Armchair nanographene, on the other hand, is expected to have a finite bandgap^{49–51} Can this result also be retrieved from our reasoning? Consider the smallest possible armchair-like nanographene approximant, phenanthrene. For this molecule, it is impossible to draw a much stabilized diradical resonance structure as was done for anthracene. The best one, the 9,10-diradical structure (Fig. 19), still has an associated energetic penalty since the loss of the aromaticity of phenanthrene (resonance energy estimated at 85 kcal/mol)⁴⁵ cannot be compensated in the same way as for anthracene by the gain in aromaticity of two benzene rings. That the transmission probability between atoms 9 and 10 is the highest of all possible phenanthrene connections is completely consistent with the detailed theoretical calculation by Yoshizawa and co-workers.¹

Since attachment of more benzene rings to this system leads to a uniform increase of the resonance energy (see the table by Wiberg;⁴⁵ +24 kcal/mol resonance energy extra per ring), this penalty will not decrease as the molecule becomes

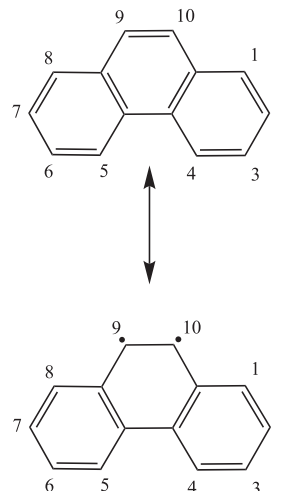


FIG. 19. Phenanthrene and one of its main (destabilized) diradical resonance structures.

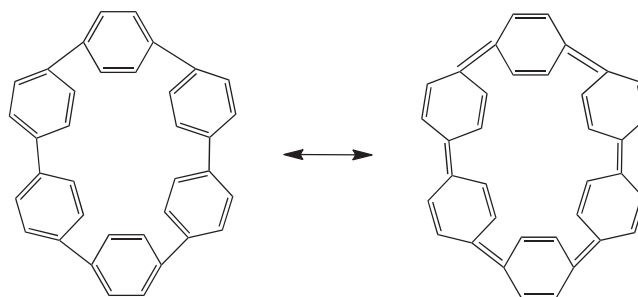
longer. For example, for picene (resonance energy estimated to be 133 kcal/mol),⁴⁵ the most stabilized diradical resonance structures (which are presented in the [supplementary material](#)) will have a similar or higher penalty than phenanthrene.

As a result, the weight of the diradical resonance structure in the resonance hybrid will remain relatively small for armchair nanoribbons (with a finite number of armchairs), leading to a low diradical character, and, associated with that, a finite bandgap. This reasoning about the difference in diradical character between zigzag and armchair nanographene is also supported by the recent work by Champagne and co-workers.⁵² The difference in band gap between zigzag and armchair nanographenes can also be understood in the light of orbital interactions.⁵³

X. OLIGOPHENYLENE MACROCYCLES

In conclusion, we consider a class of molecules that combines the two strategies presented before to modify the relative transmission, which were based on bond alternation and exploitation of aromaticity in resonance structures, respectively. Consider an oligophenylene macrocycle; a prototype of this structural type is depicted in Fig. 20. Such macrocycles have recently been synthesized.^{54–56}

The carbon atoms of the π -system in Fig. 20 hardly lie in the same plane. In reality, the macrocycle will be bent into an approximant to a circular belt, which could have an effect

FIG. 20. Cyclo-*p*-hexaphenylene with its quinoid resonance structure.

on the overlap of the p_z -orbitals of the adjacent carbon atoms. However, due to the size of the macrocycle, the resulting angle between each pair of adjacent p_z -orbitals separately will be quite moderate. Accordingly, the reasonable assumption we made is that the overlap integrals (and thus also the resonance integrals) will not be altered dramatically by the bending.

The ground state resonance hybrid of such a macrocycle has contributions from both aromatic and quinoid resonance structures. The number of aromatic resonance structures that can be drawn ($2^6 = 64$) is much higher than the number of quinoid structures (1). As such, it is likely that if all nearest-neighbor resonance integrals in this molecule are set equal, the aromatic resonance structures will swamp the quinoid structures. The net result is that it is likely that the molecule will mainly behave as an oligophenyl ring. However, it has been demonstrated experimentally that decreasing the number of benzene rings can increase the weight of the quinoidal form.^{55b,57} The strain-induced increase of the quinoidal contribution leads to an interesting dependence of the HOMO-LUMO gap on the number of the phenyl rings. Usually the more extensive π conjugation of molecules is, the smaller HOMO-LUMO gap they possess, but in the case of cyclo-*p*-phenylenes, the HOMO-LUMO gap increases as the number of phenyl rings increases.⁵⁷

Computationally the weight of the quinoid structures in the resonance hybrid can be increased by modifying the resonance integrals between the pairs of carbon atoms that carry a double bond in those structures. The effect on the transport properties of even a modest modification of the resonance integrals (e.g., a uniform modification to 0.9 for single bonds and 1.1 for double bonds in the quinoid resonance structure) is surprisingly big. For example, when contacts are placed in the way as shown in Fig. 21, the relative transmission rises from 0.004, when all resonance integrals are kept equal (polyphenylene structure), to 0.053 when the resonance integrals are modified (quinoid structure).

This behavior is easily rationalized. If the molecule could be fully described as a polyphenylene (Fig. 22, left), then the importance of the diradical resonance structures in the resonance hybrid would be low, because in order to obtain such a diradical structure, at least one aromatic ring would have to be broken. The diradical structure in which the radical centers are located on the contact positions is one of the most destabilized diradical resonance structures possible for the

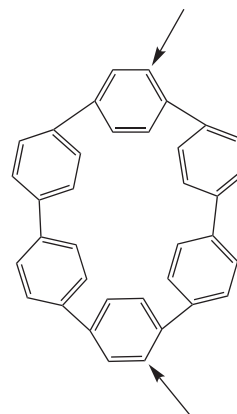


FIG. 21. Cyclo-*p*-hexaphenylene molecular electronic device with the proposed attachment sites of the contacts denoted by arrows.

considered molecule, because it demands 4 aromatic rings be broken (Fig. 22, middle).

On the other hand, if the molecule could be fully described as a “quinoid” (Fig. 22, right), the diradical structures would be more important in the resonance hybrid because these structures are “aromatically stabilized”. The more aromatic rings may be drawn in the diradical structure, the more important the structure will be (Fig. 22, middle).

Since the adjustment of the resonance integrals increases or decreases the contribution of the quinoid structures to the resonance hybrid, we can expect the relative transmission for the chosen configuration of contacts to follow suit, either increasing when the macrocycle becomes more quinoid-like or decreasing when the cycle becomes more phenylene-like. This explains qualitatively the ratio of relative transmission of 13 between the two situations studied above (0.053/0.004).

The effect can be enhanced by >2 orders of magnitude, if we could modify the resonance integrals in the “unphysical” direction, putting a bigger integral between single-bonded carbons. This will not be easy to do, but the analysis above demonstrates that the effect of perturbations to the resonance integrals/bond lengths can have spectacular effects on the relative transmission by pushing the molecule towards more or less diradical character. One could start to think that such quinoid molecules could be interesting candidates for a molecular switch.

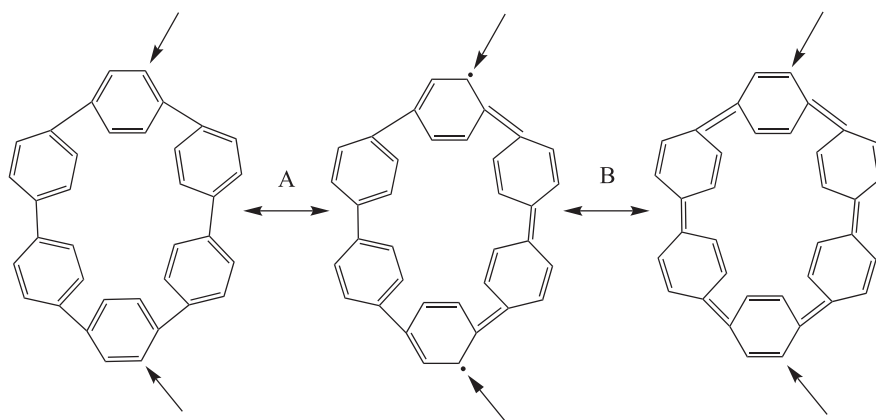


FIG. 22. (A): The “phenyl-extreme” of cyclo-*p*-hexaphenylene (left) and its (destabilized) diradical structure with the radical centers located at the contact positions (middle); (B): the “quinoid-extreme” of cyclo-*p*-hexaphenylene (right) and its (destabilized) diradical structure with the radical centers located at the contact positions (middle).

Due to sensitivity of the relative transmission to changes in the resonance integral, we can expect that even small deformations of the macrocycle will give rise to significant changes in the conductance. A straightforward way to deform a macrocycle is the application of a small mechanical force. Actually, there is an experimental observation that the application of a stretching force can affect the conductance of a molecule.⁵⁸ Another option would be side chains, which upon application of a stimulus (light, heat, and chemicals) cause a strain on the macrocycle and thus change the measured conductance. We will explore these directions in future work.

We propose polyphenylene macrocycles as a potential mechanical molecular switch. While not the first of its kind,^{59–61} and most definitely not the first molecular switch proposed,⁵⁹ this hypothetical system is a rare example of a switch that does not exploit quantum interference in its switching mechanism (i.e., no transport channels canceling each other out).^{62,63}

XI. A DIFFERENT KIND OF WIRE

In Secs. VII–X, several systems were studied which seemed to demonstrate an increase in the relative transmission (and thus also conductance) with an increasing length of the molecule. As already mentioned before, this might come across as counterintuitive and unphysical.

Usually, molecular wires are characterized through the exponential law of conductance,⁶⁴

$$G = G_0 e^{-\gamma L}, \quad (21)$$

where γ denotes the damping factor. As such, one might think that the conductance of a molecule has to decay with its length.⁶⁵ However, it has been demonstrated before that for zigzag-edge nanographenes, a so-called “reverse exponential behavior” ($\gamma < 0$) is predicted.⁶⁶ This “unusual” behavior was explained as being the result of the unique localization of the frontier orbitals on the zigzag-edges and the remarkable decrease in the HOMO-LUMO gap.⁶⁶ This can be understood by considering the orbital expression for the transmission probability in the weak interaction limit (a derivation starting from the characteristic polynomial expression can be found in the [supplementary material](#)),^{20,67,68}

$$T_{r,s}(0) = -4\tilde{\beta}^2 \left(\frac{\Delta_{rs,rs}(0)}{\Delta(0)} \right) = 4\tilde{\beta}^2 \left(\sum_k \frac{c_{rk}c_{sk}}{\varepsilon_k} \right)^2, \quad (22)$$

where c_{rk} is the MO coefficient on the r th atom in the k th MO and ε_k is the k th MO energy with respect to the Fermi energy. Both the orbital coefficients and the positioning of the energy levels depend on the size/length of the molecule. In general, the more extensive the molecule becomes, the more spread out the orbitals are, leading to smaller orbital coefficients. On the other hand, the HOMO-LUMO gap also decreases with the length of the molecule. For most molecules, the decrease in the product of orbital coefficients is faster than the decrease of the energy differences between the orbitals and the Fermi level, thus leading to an exponential decrease in the transmission probability with the length of the molecule.⁶⁹ However, when the product of the orbital coefficients on the connection sites decreases

more slowly than the decrease in HOMO-LUMO gap ($\varepsilon_k \rightarrow 0$) with increasing length of the molecule, the transmission probability at the Fermi level will rise with the length. This is just what we saw in the case of oligo(*p*-phenyl) vs. oligo(pheno)-*p*-quinodimethane molecular wires. The HOMO-LUMO gap of oligo(pheno)-*p*-quinodimethane decreases much faster than that of oligo(*p*-phenyl) as the number of phenyl rings increases (see the [supplementary material](#)). A similar argument about the balance between the HOMO-LUMO gap and the orbital coefficients as determining factors for the transmission probability was recently put forward by Proppe and Herrmann.⁸

The classical analogue of this phenomenon would be an increase in the area of a conducting wire that is bigger than the increase in the length of that wire,

$$G_{\text{classical}} = \sigma \frac{A}{l}. \quad (23)$$

The work of Tada and Yoshizawa identified nanographenes as a first example of this curious phenomenon, but as the present work demonstrates, this behavior is not restricted to those systems. We identify here several classes of molecules that have similar transport characteristics and demonstrate that this behavior is linked to the importance of the contribution of the diradical resonance structures to the resonance hybrid, enabling the use of chemical intuition to tune (and in particular, increase) the conductivity of molecules.

XII. CONCLUSIONS

In this work, an inherent measure of molecular conduction, “relative transmission,” was introduced, and its relation to transmission probability was carefully delineated. It was demonstrated that this relative transmission is related to the weight of the diradical resonance structures in the resonance hybrid. Chemical reasoning can then be marshaled to tune the conductivity of molecules by making them more or less diradical-like. We used these new insights to look at a wide variety of conjugated alternant hydrocarbons and were able to rationalize their transport properties. Molecular chains can, in quite specific and understood circumstances, become more conductive the longer they get, in contradiction to what might have been expected intuitively. The effect is strikingly demonstrated in oligo(pheno)-*p*-quinodimethane chains. The proposal of a new potential molecular switch (utilizing oligo-*p*-phenylene macrocycles) arises from our considerations.

SUPPLEMENTARY MATERIAL

See [supplementary material](#) for a detailed recap of the SSP method, the computational details, the detailed VB and NEGF-DFT calculations, the diradical resonance structures for anthracene and picene, the derivation of Eq. (22), and the application of our new insights to cyclobutadiene.

ACKNOWLEDGMENTS

We are grateful to J. Gu, W. Wu, D. Danovich, and S. Shaik for sharing their VB calculations on polyenes with

us, and for providing new calculations. We are grateful to a careful reviewer of our paper, and to S. Gansekaran and L. Venkataraman for their comments. T.S. acknowledges the Research Foundation-Flanders (FWO) for a position as research assistant (Grant No. 11ZG615N). S.F. wishes to thank the Research Foundation-Flanders (FWO) for financial support for his postdoctoral research in the General Chemistry (Algemene Chemie, ALGC)) group. P.G. and F.D.P. wish to acknowledge the VUB for a Strategic Research Program. The research at Cornell was supported by the National Science Foundation through Research Grant No. CHE-1305872. We thank C. Herrmann for furnishing her useful Artaios program to us.

APPENDIX: COMPUTATIONAL DETAILS

An in-house program was developed to calculate relative transmissions. In general, the simple Hückel theory was used to construct the Hamiltonian matrices ($\beta = 1$), unless the resonance integrals have been adjusted. Whenever this is the case, the exact values of the resonance integrals will be mentioned. A PYTHON code inverts the Hückel Hamiltonian matrices. The elements of this inverse matrix can be related to the relative transmission (see the [supplementary material](#)).

The DFT calculations on the molecular wires were performed using the Non-Equilibrium Green's Function (NEGF) method combined with DFT as it is implemented in the Artaios code:^{70,71} a postprocessing tool for Gaussian 09.⁷² Gold (111) surfaces were chosen as the electrodes and thiol ($-\text{SH}$) as an anchor unit to connect the molecules to the contacts. To avoid steric hindrance between the bridged molecule and the electrode surface, an ethynyl spacer ($-\text{C}\equiv\text{C}-$) was added between the molecule and the thiol anchor unit. The resulting molecular structures are shown in the [supplementary material](#). In the first step, the examined structures were optimized at the B3LYP⁷³/6-31G(d) level of theory, as implemented in the Gaussian 09 software. After this optimization, the thiol's hydrogen atoms were removed and Au_9 clusters, approximating the electrode surface, were attached in accordance with the methodology presented in a recent study.⁷⁴ The adsorption site is the fcc-hollow site. The Au-S distance was set to 2.48 Å.⁷⁵ For the resulting structures, single-point calculations were performed at the B3LYP/LanL2DZ level of theory, again using the Gaussian 09 software. In the final step, the Hamiltonian and overlap matrices were extracted to carry out the NEGF calculation within the wide-band-limit (WBL) approximation using the post-processing tool Artaios.⁷⁶ In the WBL approximation, we used a constant value of 0.036 eV^{-1} for the local density of states (LDOS) of the electrode surface. This value was taken from the literature.⁷⁶

¹K. Yoshizawa, T. Tada, and A. Staykov, *J. Am. Chem. Soc.* **130**, 9406 (2008).

²Y. Tsuji and R. Hoffmann, *Angew. Chem., Int. Ed.* **126**, 4177 (2014).

³G. C. Solomon, D. Q. Andrews, T. Hansen, R. H. Goldsmith, M. R. Wasielewski, R. P. Van Duyne, and M. A. Ratner, *J. Chem. Phys.* **129**, 054701 (2008).

⁴T. Markussen, R. Stadler, and K. S. Thygesen, *Nano Lett.* **10**, 4260 (2010).

⁵N. Ramos-Berdullas and M. Mandado, *Chem. - Eur. J.* **19**, 3646 (2013).

⁶T. Stuyver, S. Fias, F. De Proft, and P. Geerlings, *Chem. Phys. Lett.* **630**, 51 (2015).

⁷D. Mayou, Y. Zhou, and M. Ernzerhof, *J. Phys. Chem. C* **117**, 7870 (2013).

⁸J. Proppe and C. Herrmann, *J. Comput. Chem.* **36**, 201 (2015).

⁹F. H. Burkitt, C. A. Coulson, and H. C. Longuet-Higgins, *Trans. Faraday Soc.* **47**, 553 (1951).

¹⁰F. Goyer, M. Ernzerhof, and M. Zhuang, *J. Chem. Phys.* **126**, 144104 (2007).

¹¹B. T. Pickup and P. W. Fowler, *Chem. Phys. Lett.* **459**, 198 (2008).

¹²P. W. Fowler, B. T. Pickup, T. Z. Todorova, and W. J. Myrvold, *Chem. Phys.* **131**, 044104 (2009).

¹³S. Datta, *Electronic Transport in Mesoscopic Systems* (Cambridge University Press, 1997).

¹⁴P. W. Fowler, B. T. Pickup, and T. Z. Todorova, *Pure Appl. Chem.* **83**, 1515 (2011).

¹⁵C. A. Coulson and H. C. Longuet-Higgins, *Proc. R. Soc. A* **192**, 16 (1947).

¹⁶T. Stuyver, S. Fias, F. De Proft, P. W. Fowler, and P. Geerlings, *J. Chem. Phys.* **142**, 094103 (2015).

¹⁷Y. Tsuji, R. Hoffmann, M. Strange, and G. C. Solomon, *Proc. Natl. Acad. Sci. U. S. A.* **113**, E413 (2016).

¹⁸P. W. Fowler, B. T. Pickup, T. Z. Todorova, and W. J. Myrvold, *Chem. Phys.* **131**, 244110 (2009).

¹⁹H. Hosoya and K. Hosoi, *J. Chem. Phys.* **64**, 1065 (1976).

²⁰N. S. Ham, *J. Chem. Phys.* **29**, 1229 (1958).

²¹E. Heilbronner, *Helv. Chim. Acta* **45**, 1722 (1962).

²²L. N. Trefethen and D. Bau, *Numerical Linear Algebra* (SIAM, 1997).

²³C. F. Wilcox, Jr., *Tetrahedron Lett.* **7**, 795–800 (1968).

²⁴M. J. S. Dewar and H. C. Longuet-Higgins, *Proc. R. Soc. A* **214**, 482–493 (1952).

²⁵I. Gutman, *J. Chem. Soc., Faraday Trans.* **89**, 2413–2416 (1993).

²⁶T. Stuyver, S. Fias, F. De Proft, and P. Geerlings, *J. Phys. Chem. C* **119**, 26390 (2015).

²⁷A. E. Taylor, *Am. Math. Mon.* **59**, 20–24 (1952).

²⁸T. Bally and W. T. Borden, *Reviews in Computational Chemistry* (Wiley, 2007), Vol. 13; W. T. Borden, *Diradicals* (Wiley, 1982).

²⁹J. Michl and V. Bonačić-Koutecký, *Electronic Aspects of Organic Photochemistry* (Wiley, 1990).

³⁰H. A. Jahn and E. Teller, *Proc. R. Soc. London, Ser. A* **161**, 220 (1937).

³¹L. Pauling, *The Chemical Bond: A Brief Introduction to Modern Structural Chemistry* (Cornell University Press, 1967).

³²M. Abe, *Chem. Rev.* **113**, 7011 (2013).

³³Y. Tsuji, R. Movassagh, S. Datta, and R. Hoffmann, *ACS Nano* **9**, 11109 (2015).

³⁴A. C. Benniston, V. Goulle, A. Harriman, J.-M. Lehn, and B. Marczinke, *J. Phys. Chem.* **98**, 7798 (1994).

³⁵A. Osuka, N. Tanabe, S. Kawabata, I. Yamazaki, and Y. Nishimura, *J. Org. Chem.* **60**, 7177 (1995).

³⁶S. S. Shaik and P. C. Hiberty, *A Chemist's Guide to Valence Bond Theory* (John Wiley & Sons, 2007).

³⁷J. Gu, W. Wu, and S. S. Shaik, private communication (2016).

³⁸W. Wu, D. Danovich, A. Shurki, and S. Shaik, *J. Phys. Chem. A* **104**, 8744–8758 (2000); J. Gu, Y. Lin, B. Ma, W. Wu, and S. Shaik, *J. Chem. Theory Comput.* **4**, 2101–2107 (2008).

³⁹S. S. Shaik and D. Danovich, private communication (2016).

⁴⁰M. Nakano, R. Kishi, T. Nitta, T. Kubo, K. Nakasui, K. Kamada, K. Ohta, B. Champagne, E. Botek, and K. Yamaguchi, *J. Phys. Chem. A* **109**, 885 (2005).

⁴¹Y. Geng, S. Sangtarash, C. Huang, H. Sadeghi, Y. Fu, W. Hong, T. Wandlowski, S. Decurtins, C. J. Lambert, and S. Liu, *J. Am. Chem. Soc.* **137**, 4469 (2015).

⁴²R. Frisenda, M. L. Perrin, H. Valkenier, J. C. Hummelen, and H. S. van der Zant, *Phys. Status Solidi B* **250**, 2431 (2013).

⁴³V. Kaliginedi, P. Moreno-García, H. Valkenier, W. Hong, V. M. García-Suárez, P. Buitter, J. L. H. Otten, J. C. Hummelen, C. J. Lambert, and T. Wandlowski, *J. Am. Chem. Soc.* **134**, 5262 (2012).

⁴⁴C. A. Coulson, *Valence* (Clarendon Press, 1953).

⁴⁵K. B. Wiberg, *J. Org. Chem.* **62**, 5720 (1997).

⁴⁶J. R. Dias, *J. Phys. Chem. A* **117**, 4716 (2013).

⁴⁷J. R. Dias, *Croat. Chem. Acta* **86**, 379 (2013).

⁴⁸J. Hachmann, J. J. Dorando, M. Avilés, and G. K.-L. Chan, *J. Chem. Phys.* **127**, 134309 (2007).

⁴⁹A. C. Neto, F. Guinea, N. M. Peres, K. S. Novoselov, and A. K. Geim, *Rev. Mod. Phys.* **81**, 109 (2009).

⁵⁰K. A. Ritter and J. W. Lyding, *Nat. Mater.* **8**, 235 (2009).

⁵¹F. J. Martin-Martinez, S. Fias, G. Van Lier, F. De Proft, and P. Geerlings, *Chem. - Eur. J.* **18**, 6183 (2012).

⁵²A. Shimizu, Y. Hirao, T. Kubo, M. Nakano, E. Botek, and B. T. Champagne, *AIP Conf. Proc.* **1504**, 399 (2012).

- ⁵³K. Yoshizawa, K. Yahara, K. Tanaka, and T. Yamabe, *J. Phys. Chem. B* **102**, 498 (1998).
- ⁵⁴R. Jasti, J. Bhattacharjee, J. B. Neaton, and C. R. Bertozzi, *J. Am. Chem. Soc.* **130**, 17646 (2008); T. J. Sisto, M. R. Golder, E. S. Hirst, and R. Jasti, *ibid.* **133**, 15800 (2011); J. Xia and R. Jasti, *Angew. Chem., Int. Ed.* **51**, 2474 (2012); E. R. Darzi, T. J. Sisto, and R. Jasti, *J. Org. Chem.* **77**, 6624 (2012); J. Xia, J. W. Bacon, and R. Jasti, *Chem. Sci.* **3**, 3018 (2012); P. J. Evans, E. R. Darzi, and R. Jasti, *Nat. Chem.* **6**, 404 (2014).
- ⁵⁵(a) H. Takaba, H. Omachi, Y. Yamamoto, J. Bouffard, and K. Itami, *Angew. Chem., Int. Ed.* **48**, 6112 (2009); (b) H. Omachi, S. Matsuura, Y. Segawa, and K. Itami, *ibid.* **49**, 10202 (2010); (c) Y. Segawa, S. Miyamoto, H. Omachi, S. Matsuura, P. Šenel, T. Sasamori, N. Tokitoh, and K. Itami, *ibid.* **50**, 3244 (2011); (d) Y. Segawa, P. Šenel, S. Matsuura, H. Omachi, and K. Itami, *Chem. Lett.* **40**, 423 (2011); (e) Y. Ishii, Y. Nakanishi, H. Omachi, S. Matsuura, K. Matsui, H. Shinohara, Y. Segawa, and K. Itami, *Chem. Sci.* **3**, 2340 (2012); (f) F. Sibbel, K. Matsui, Y. Segawa, A. Studer, and K. Itami, *Chem. Commun.* **50**, 954 (2014); (g) Y. Segawa, T. Kuwabara, K. Matsui, S. Kawai, and K. Itami, *Tetrahedron* **26**, 4500 (2015).
- ⁵⁶S. Yamago, Y. Watanabe, and T. Iwamoto, *Angew. Chem., Int. Ed.* **49**, 757 (2010); T. Iwamoto, Y. Watanabe, Y. Sakamoto, T. Suzuki, and S. Yamago, *J. Am. Chem. Soc.* **133**, 8354 (2011); E. Kayahara, Y. Sakamoto, T. Suzuki, and S. Yamago, *Org. Lett.* **14**, 3284 (2012); E. Kayahara, T. Iwamoto, T. Suzuki, and S. Yamago, *Chem. Lett.* **42**, 621 (2013); E. Kayahara, V. K. Patel, and S. Yamago, *J. Am. Chem. Soc.* **136**, 2284 (2014); E. Kayahara, V. K. Patel, J. Xia, R. Jasti, and S. Yamago, *Synlett* **26**, 1615 (2015); V. K. Patel, E. Kayahara, and S. Yamago, *Chem. - Eur. J.* **21**, 5742 (2015).
- ⁵⁷E. Kayahara, T. Kouyama, T. Kato, and S. Yamago, *J. Am. Chem. Soc.* **138**, 338 (2016).
- ⁵⁸B. Q. Xu, X. L. Li, X. Y. Xiao, H. Sakaguchi, and N. J. Tao, *Nano Lett.* **5**, 1491 (2005).
- ⁵⁹L. Sun, Y. A. Diaz-Fernandez, T. A. Geschneidner, F. Westerlund, S. Lara-Avila, and K. Moth-Poulsen, *Chem. Soc. Rev.* **43**, 7378 (2014).
- ⁶⁰R. Frisenda, V. A. Janssen, F. C. Grozema, H. S. van der Zant, and N. Renaud, *Nat. Chem.* **8**, 1099 (2016).
- ⁶¹S. Y. Quek, M. Kamenetska, M. L. Steigerwald, H. J. Choi, S. G. Louie, M. S. Hybertsen, J. B. Neaton, and L. Venkataraman, *Nat. Nanotech.* **4**, 230 (2009).
- ⁶²A. Staykov, M. Watanabe, T. Ishihara, and K. Yoshizawa, *J. Phys. Chem. C* **118**, 27539 (2014).
- ⁶³T. Toyama, K. Higashiguchi, T. Nakamura, H. Yamaguchi, E. Kusaka, and K. Matsuda, *J. Phys. Chem. Lett.* **7**, 2113 (2016).
- ⁶⁴M. Magoga and C. Joachim, *Phys. Rev. B* **56**, 4722 (1997).
- ⁶⁵V. Mujica, M. Kemp, and M. A. Ratner, *J. Chem. Phys.* **101**, 6856 (1994).
- ⁶⁶T. Tada and K. Yoshizawa, *J. Phys. Chem. B* **108**, 7565 (2004).
- ⁶⁷N. S. Ham and K. Ruedenberg, *J. Chem. Phys.* **29**, 1215–1229 (1952).
- ⁶⁸I. Gutman, *MATCH Commun. Math. Comput. Chem.* **56**, 345 (2006).
- ⁶⁹T. Tada and K. Yoshizawa, *Phys. Chem. Chem. Phys.* **17**, 32099 (2015).
- ⁷⁰C. Herrmann, G. C. Solomon, J. E. Subotnik, V. Mujica, and M. A. Ratner, *J. Chem. Phys.* **132**, 024103 (2010).
- ⁷¹C. Hermann, L. Gross, T. Steenbock, and G. C. Solomon, “Artaios—A code for postprocessing quantum chemical electronic structure calculations,” Report (2010–2014).
- ⁷²M. J. Frisch, G. W. Trucks, H. B. Schlegel, G. E. Scuseria, M. A. Robb, J. R. Cheeseman, G. Scalmani, V. Barone, B. Mennucci, G. A. Petersson, H. Nakatsuji, M. Caricato, X. Li, H. P. Hratchian, A. F. Izmaylov, J. Bloino, G. Zheng, J. L. Sonnenberg, M. Hada, M. Ehara, K. Toyota, R. Fukuda, J. Hasegawa, M. Ishida, T. Nakajima, Y. Honda, O. Kitao, H. Nakai, T. Vreven, J. A. Montgomery, Jr., J. E. Peralta, F. Ogliaro, M. Bearpark, J. J. Heyd, E. Brothers, K. N. Kudin, V. N. Staroverov, R. Kobayashi, J. Normand, K. Raghavachari, A. Rendell, J. C. Burant, S. S. Lyengar, J. Tomasi, M. Cossi, N. Rega, J.M. Millam, M. Klene, J. E. Knox, J. B. Cross, V. Bakken, C. Adamo, J. Jaramillo, R. Gomperts, R. E. Stratmann, O. Yazyev, A. J. Austin, R. Cammi, C. Pomelli, J. W. Ochterski, R. L. Martin, K. Morokuma, V. G. Zakrzewski, G. A. Voth, P. Salvador, J. J. Danenberg, S. Dapprich, A. D. Daniels, Ö. Farkas, J. B. Fisman, J. V. Ortiz, J. Cioslowski, and D. J. Fox, *GAUSSIAN 09*, Revision D.01, Gaussian Inc., 2009.
- ⁷³A. D. Becke, *Phys. Rev. A* **38**, 3098 (1988); C. Lee, W. Yang, and R. G. Parr, *ibid.* **37**, 785 (1988); A. D. Becke, *J. Chem. Phys.* **98**, 5648 (1993); P. J. Stephens, F. J. Devlin, C. F. Chabalowski, and M. J. Frisch, *J. Phys. Chem.* **98**, 11623 (1994).
- ⁷⁴H. Schlicke and C. Herrmann, *ChemPhysChem* **15**, 4011 (2014).
- ⁷⁵A. Bilić, J. R. Reimers, and N. S. Hush, *J. Chem. Phys.* **122**, 094708 (2005).
- ⁷⁶C. Herrmann, G. C. Solomon, and M. A. Ratner, *J. Chem. Phys.* **134**, 224306 (2011).